J|A|C|S
COMMUNICATIONS

Published on Web 03/04/2006

Stable Photogenerated Carriers in Magnetic Semiconductor Nanocrystals

William K. Liu, Kelly M. Whitaker, Kevin R. Kittilstved, and Daniel R. Gamelin*

Department of Chemistry, University of Washington, Seattle, Washington 98195-1700

Received January 20, 2006; E-mail: gamelin@chem.washington.edu

The generation and manipulation of electron spins in magnetic semiconductor nanostructures is a central theme of the emerging field of spintronics.[1] Spin valves and spin-based light-emitting diodes have been demonstrated using diluted magnetic semiconductor (DMS)[2] nanostructures grown by molecular beam epitaxy.[1,3] The novel functionalities of these spintronics devices derive from carrier−dopant magnetic exchange interactions in the DMSs. In this communication, we report the preparation of colloidal DMS nanocrystals possessing additional quantum-confined conduction band (CB) electrons and describe the use of electron paramagnetic resonance (EPR) spectroscopy to probe the coupling between these electrons and the magnetic dopants. Although charged[4−6] and magnetically doped[7] colloidal semiconductor nanocrystals have been reported separately, colloidal nanocrystals that have been both charged and magnetically doped as described herein have not. This new motif presents unexplored opportunities for investigation of carrier−dopant interactions in DMS nanostructures important to many magneto-electronic phenomena, including carrier-mediated ferromagnetism, magnetic polaron nucleation, and proposed spin-based quantum information processing schemes.

Alkyl-capped ZnO and TM^{2+}-doped ZnO ($TM^{2+} = Co^{2+}$, Mn^{2+}) nanocrystals suspended in toluene were prepared and characterized as described previously.[8,9] These colloids were reduced photochemically by ultraviolet (UV) laser irradiation in the presence of EtOH, a hole quencher[4] (see Supporting Information for experimental details). Figure 1a,b shows 298 K electronic absorption spectra of 2.6% Co^{2+}:ZnO nanocrystals suspended in toluene in their as-prepared and reduced forms. With reduction, the first excitonic peak in the UV was bleached, and an intense near-infrared (NIR) band appeared, as reported previously for pure ZnO colloids.[5] The UV bleaching has been attributed to partial filling of the CB and the new NIR intensity to dipole-allowed intra-CB transitions.[5,6] Together, these spectral changes are the signature of CB electrons (e^-_{CB}).[10]

Figure 1c,e shows 298 K electronic absorption spectra of concentrated suspensions of 4.2% Co^{2+}:ZnO and 0.8% Mn^{2+}:ZnO colloids in toluene in their as-prepared and reduced forms. The sub-bandgap absorption spectra of the as-prepared DMS nanocrystals have been described previously.[8,9] With photoreduction, both suspensions exhibited the signature UV bleaching and NIR absorption (e.g., Figure 1a,b). For Co^{2+}:ZnO, the difference spectrum (reduced − as-prepared, Figure 1d) shows no other features. Notably, there was no detectable change in the $^4A_2 \rightarrow {}^4T_1(P)$ or $^4T_1(F)$ intensities centered at 16 500 and 7200 cm^{-1}, respectively (ΔAbs < 0.8%), demonstrating that Co^+ is not formed at appreciable concentrations under these conditions (Co^+ cation mole fraction < 0.03%). Because the as-prepared Co^{2+}:ZnO nanocrystals are already blue from the $^4A_2 \rightarrow {}^4T_1(P)$ ligand field absorption, they do not color significantly upon reduction.

For Mn^{2+}:ZnO, bleaching was also observed at ~24 000 cm^{-1} upon photoreduction (Figure 1e,f). Absorption and magnetic circular dichroism spectroscopies have previously identified the 24 000 cm^{-1} band as a donor-type photoionization transition involving promotion of a Mn^{2+} electron into the CB.[9] Bleaching of this $Mn^{2+} \rightarrow$ CB transition is consistent with CB filling and may also reflect suppression of its intensity-stealing mechanism, which involves configuration interaction with the nearby excitonic levels.[11] The spectral changes in Figure 1e result in coloration of the Mn^{2+}:ZnO nanocrystals from yellow/brown (as-prepared) to emerald green (reduced). In all cases, the reduced nanocrystals were stable indefinitely (k_{decay} < 0.01/week at 298 K) when kept anaerobic but returned rapidly to their original forms upon exposure to air (gray dots in Figure 1), consistent with facile reoxidation.

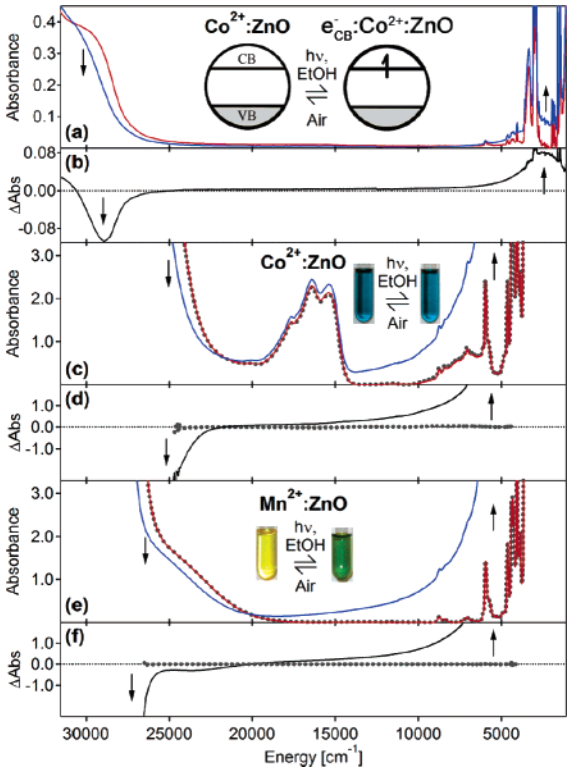

Figure 1. The 298 K absorption (a, c, e) and difference absorption (b, d, f) spectra of 4.5 ± 0.2 nm diameter nanocrystals: as-prepared (red line), photoreduced (blue line), and reoxidized (gray dotted line): (a, b) 2.6% Co^{2+}:ZnO, dilute; (c, d) 4.2% Co^{2+}:ZnO, concentrated; (e, f) 0.8% Mn^{2+}:ZnO, concentrated.

EPR spectroscopy was also used to study the reduced nanocrystals. Figure 2a shows 298 K EPR spectra of as-prepared and reduced colloidal ZnO nanocrystals. The as-prepared ZnO nanocrystals showed no EPR signal. A new $g = 1.96$ signal was detected after photoreduction (Figure 2a) similar to that reported for shallow donors in nanocrystalline ZnO.[12,13] The deviation of this resonance from $g = 2.00$ indicates that it does not derive from deep donors, such as surface traps, and previous investigations[12] of shallow donor EPR signals have demonstrated that $g = 1.96$ is in fact predicted for e^-_{CB} from $K \cdot P$ treatment of the ZnO band structure, confirming the band character of the photogenerated electron in Figure 2a. A more detailed description of this EPR spectrum for ZnO nano-

10.1021/ja060488p CCC: $33.50

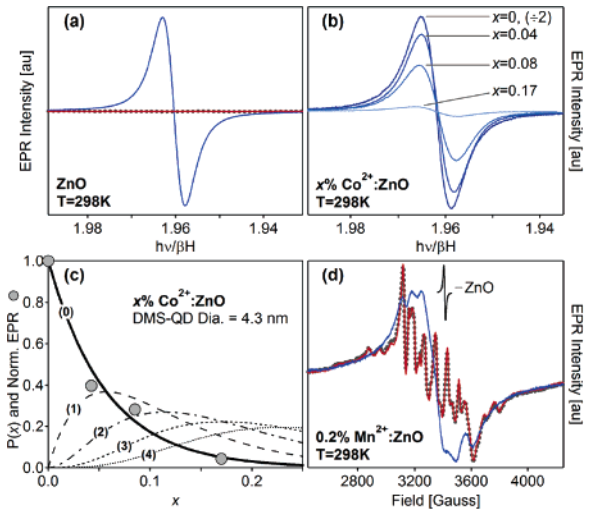

Figure 2. The 298 K EPR spectra of as-prepared (red line), reduced (blue line), and reoxidized (gray dotted line) colloidal nanocrystals: (a) ~4.1 nm diameter ZnO nanocrystals; (b) ~4.3 nm diameter *x* % Co^{2+}:ZnO nanocrystals after photoreduction; (c) EPR intensity from part (b) plotted versus *x*. Curves show statistical probabilities calculated for 0−4 dopants/particle; (d) ~8.0 nm diameter 0.2% Mn^{2+}:ZnO nanocrystals, with inset showing the reduced ZnO EPR spectrum from part (a) on the same *x* axis.

crystals is beyond the scope of the present communication and will be presented elsewhere.

Figure 2b shows 298 K EPR spectra of as-prepared and reduced Co^{2+}:ZnO nanocrystals at various Co^{2+} cation percent mole fractions (*x*). At 298 K, as-prepared Co^{2+}:ZnO shows no EPR signal due to rapid Co^{2+} spin−lattice relaxation,[14] making this system amenable to observation of e^-_{CB} upon photoreduction. For small *x*, a $g = 1.96$ EPR signal was detected after photoreduction (Figure 2b) identical to the one observed in Figure 2a. With increasing *x*, this EPR signal weakened substantially, despite clear evidence of nanocrystal reduction from absorption spectroscopy (e.g., Figure 1a−d). A plot of EPR intensity versus *x* (Figure 2c) for a series of nanocrystals reduced under identical conditions reveals that the EPR intensity correlates quantitatively with the fraction of undoped ZnO nanocrystals calculated from Poisson statistics.[7] A single Co^{2+} ion thus completely suppresses the e^-_{CB} EPR signal under these conditions, likely by lifetime broadening due to $Co^{2+}-e^-_{CB}$ coupling.

$$|N_0\alpha| = \left|\frac{\Delta E}{x\langle S_z\rangle}\right| \approx \left|\frac{\langle n\rangle \Delta\Gamma}{x\langle S_z\rangle}\right| \qquad (1)$$

Figure 2d shows EPR spectra of as-prepared and reduced 0.2% Mn^{2+}:ZnO nanocrystals. In contrast with Co^{2+}, Mn^{2+} in ZnO relaxes slowly[14] and shows a strong EPR signal at 298 K with extensive hyperfine structure described by the axial spin Hamiltonian parameters $g_{iso} = 1.999$, $A_{iso} = -74.0 \times 10^{-4}$ cm^{-1}, and $D = -2.36 \times 10^{-2}$ cm^{-1}.[9] This structure broadened substantially upon reduction, a change that was quantitatively reversed by exposure to air (dotted line in Figure 2d). Importantly, the spectrum of reduced Mn^{2+}:ZnO nanocrystals is not the simple sum of Mn^{2+} and e^-_{CB} spectra, indicating substantial $Mn^{2+}-e^-_{CB}$ interaction. To estimate the effective (mean-field) $Mn^{2+}-e^-_{CB}$ exchange energy, the line broadening of Figure 2d was analyzed. Assuming the Mn^{2+} line broadening ($\Delta\Gamma$) arises solely from exchange splitting of each Mn^{2+} hyperfine peak by interaction with the $S = {}^1/_2$ e^-_{CB}, a mean Mn^{2+} level splitting of 40 G (0.23 μeV or 1.9×10^{-3} cm^{-1}) is estimated. The total exchange energy experienced by e^-_{CB} is the sum over all $Mn^{2+}-e^-_{CB}$ interactions. For 8.0 nm diameter 0.2% Mn^{2+}:ZnO nanocrystals, the mean Mn^{2+} occupancy is $\langle n\rangle = 22.5$, so $\Delta E(e^-_{CB}) \approx 4.3 \times 10^{-2}$ cm^{-1}. This result can be related to the mean-field exchange parameter $N_0\alpha$ typically used to describe $TM^{2+}-e^-_{CB}$ coupling in bulk DMSs[2] via eq 1, where $|\langle S_z\rangle| = 0.004$ is the Mn^{2+} spin expectation value under the experimental conditions of 298 K and ~0.33 T used for Figure 2d. Solving eq 1 yields $|N_0\alpha| \approx 0.66$ eV, a value comparable to those reported[2] for bulk Mn^{2+}:ZnSe (+0.26 eV), Mn^{2+}:ZnTe (+0.18 eV), and Mn^{2+}:CdSe (+0.26 eV), as well as that used to model magneto-transport in Mn^{2+}:ZnO films (+0.19 eV).[15] Although reasonable in magnitude, this experimental estimate neglects Mn^{2+} relaxation broadening[16] and makes no attempt to account for nonstatistical dopant distributions,[7,8] carrier-mediated $Mn^{2+}-Mn^{2+}$ exchange coupling,[15] or nanocrystal overcharging,[6] all of which should be important variables. Future experiments will seek to address these variables in order to refine the estimate of $N_0\alpha$. Nevertheless, the data in Figure 2 clearly demonstrate both the existence of $TM^{2+}-e^-_{CB}$ exchange interactions in charged DMS nanocrystals and the possibility to study these interactions spectroscopically.

In summary, CB electrons have been successfully introduced into colloidal diluted magnetic semiconductor nanocrystals, and manifestations of $TM^{2+}-e^-_{CB}$ interactions have been observed by EPR spectroscopy. This new motif of colloidal charged magnetic semiconductor nanocrystals presents attractive new opportunities for studying and potentially manipulating spins in quantum-confined nanostructures prepared by direct chemical methods. Extension of this research to other DMSs and nanocrystal dimensionalities is expected to reveal interesting new phenomena relevant to future spin-based information processing applications.

Acknowledgment. This work was funded by the NSF (DMR-0239325 to D.R.G. and DGE-0504573 (IGERT fellowship) to K.M.W.), the Research Corporation, and the Dreyfus Foundation. The authors thank Prof. Bruce Robinson and Alyssa Smith for stimulating discussions.

Supporting Information Available: Experimental details and additional luminescence spectra. This material is available free of charge via the Internet at http://pubs.acs.org.

References

(1) Wolf, S. A.; Awschalom, D. D.; Buhrman, R. A.; Daughton, J. M.; von Molnár, S.; Roukes, M. L.; Chthelkanova, A. Y.; Treger, D. M. *Science* **2001**, *294*, 1488.
(2) Furdyna, J. K. *J. Appl. Phys.* **1988**, *64*, R29.
(3) (a) Rüster, C.; Borzenko, T.; Gould, C.; Schmidt, G.; Molenkamp, L. W.; Liu, X.; Wojtowicz, T. H.; Furdyna, J. K.; Yu, Z. G.; Flatté, M. E. *Phys. Rev. Lett.* **2003**, *91*, 216602. (b) Jonker, B. T.; Park, Y. D.; Bennett, B. R.; Cheong, H. D.; Kioseoglou, G.; Petrou, A. *Phys. Rev. B* **2000**, *62*, 8180.
(4) Hasse, M.; Weller, H.; Henglein, A. *J. Phys. Chem.* **1988**, *92*, 482.
(5) (a) Shim, M.; Guyot-Sionnest, P. *J. Am. Chem. Soc.* **2001**, *123*, 11651. (b) Shim, M.; Guyot-Sionnest, P. *Nature* **2000**, *407*, 981.
(6) Garmeau, A.; Roest, A. L.; Vanmaekelbergh, D.; Allan, G.; Delerue, C.; Meulenkamp, E. A. *Phys. Rev. Lett.* **2003**, *90*, 097401.
(7) For a recent review, see: Bryan, J. D.; Gamelin, D. R. *Prog. Inorg. Chem.* **2005**, *54*, 47.
(8) Schwartz, D. A.; Norberg, N. S.; Nguyen, Q. P.; Parker, J. M.; Gamelin, D. R. *J. Am. Chem. Soc.* **2003**, *125*, 13205.
(9) Norberg, N. S.; Kittilstved, K. R.; Amonette, J. E.; Kukkadapu, R. K.; Schwartz, D. A.; Gamelin, D. R. *J. Am. Chem. Soc.* **2004**, *126*, 9387.
(10) One electron in a 4.5 nm diameter nanocrystal corresponds to a carrier concentration of 2.1×10^{19} cm^{-3}.
(11) Liu, W.; Salley, G. M.; Gamelin, D. R. *J. Phys. Chem. B* **2005**, *109*, 14486.
(12) Zhou, H.; Hofstaetter, A.; Hoffman, D. M.; Meyer, B. K. *Microelectron. Eng.* **2003**, *66*, 59.
(13) Orlinskii, S. B.; Schmidt, J.; Baranov, P. G.; Hofmann, D. M.; de Mello Donega, C.; Meijerink, A. *Phys. Rev. Lett.* **2004**, *92*, 047603.
(14) Mabbs, F. E.; Collison, D. *Electron Paramagnetic Resonance of d Transition Metal Compounds*; Elsevier: Amsterdam, 1992.
(15) Andrearczyk, T.; Jaroszy'nski, J.; Grabecki, G.; Dietl, T.; Fukumura, T.; Kawasaki, M. *Phys. Rev. B* **2005**, *72*, 121309.
(16) Milivojevic, D.; Babic Stojic, B.; Stojic, M.; Kulbachinskii, V. A.; Maryanchuk, P. D.; Churilov, I. A. *Solid State Commun.* **2002**, *122*, 389.

JA060488P